Histol Histopathol (2021) 36: 1063-1072

http://www.hh.um.es

Histology and Histopathology
From Cell Biology to Tissue Engineering

ORIGINAL ARTICLE **Open Access**

LncRNA ADAMTS9-AS1 knockdown restricts cell proliferation and EMT in non-small cell lung cancer

Zhongwen Li, Guojun Yue, Tingyou Zhang, Jinzhi Wu and Xin Tian

Department of Oncology, The Second Affiliated Hospital of Zunyi Medical University, Zunyi, Guizhou, PR China

Summary. A recent bioinformatics analysis identified long non-coding RNA antisense 1 ADAMTS9-AS1 as an independent prognostic marker in several tumors, including prostate cancer and bladder cancer. Nevertheless, the prognostic value and functional role of ADAMTS9-AS1 in non-small cell lung cancer (NSCLC) remain elusive. Here, we first found that the expression of ADAMTS9-AS1 was significantly upregulated in NSCLC tissues compared with adjacent normal tissues using quantitative real time PCR analysis. Clinically, we observed that ADAMTS9-AS1 expression was associated with TNM stage, lymph node metastasis and poor prognosis in NSCLC patients. By performing loss-of-function assay in A549 and 95D cells, our *in vitro* experiments further showed that knockdown of ADAMTS9-AS1 remarkedly suppressed cell proliferation, caused cell cycle G0/G1 arrest and apoptosis, and inhibited cell migration and invasion in NSCLC cells using CCK-8, colony formation, flow cytometry and transwell assays. Moreover, we found that ADAMTS9-AS1 knockdown downregulated the expression of CDK4, N-cadherin, Vimentin, but upregulated the expression of Bad and E-cadherin. In summary, our results revealed that ADAMTS9-AS1 may serve as a potential therapeutic target for the treatment of patients with NSCLC.

Key words: ADAMTS9-AS1, NSCLC, Prognosis, Proliferation, EMT

Introduction

Lung cancer is one of the frequent malignancies with nearly 2.1 million new cases and 1.8 deaths in 2018 alone over all the world (Cai and Liu, 2019), of which non-small cell lung cancer (NSCLC) is identified as the major subtype, accounting for approximately 85% of lung cancer cases (Pao and Chmielecki, 2010). Although considerable progress has been made in treatment methods, including surgical resection, chemotherapy or radiotherapy, the five-year survival rate still remains lower than 20% with a high rate of local recurrence and metastasis (Crino et al., 2010; Didkowska et al., 2016; Hirsch et al., 2017). Therefore, it is urgently required to investigate the underlying mechanisms of the occurrence and development of NSCLC to develop therapeutic strategies against this disease.

Long non-coding RNAs (lncRNAs) with a length of more than 200 nucleotides have gradually become important regulators of the development of cancer progression by modulating various biological activities such as cell growth, proliferation, apoptosis and metastasis (Hui et al., 2019; Xu et al., 2019a,b; Yang et al., 2019). There are increasing studies that have shown that lncRNAs are aberrantly expressed in NSCLC by serving as oncogenes or tumor suppressors. For instance, lncRNA CASC19 was upregulated in NSCLC and accelerates the progression of NSCLC by regulating the proliferation, migration and invasion of tumor cells (Qu et al., 2019). Similarly, Chen and Wang (2019) reported that lncRNA ZEB2-AS1 significantly elevated the viability and malignant degree of NSCLC cells, thus aggravating the development of NSCLC. Conversely, lncRNA BX357664 was lowly-expressed in NSCLC tissues, which not only predicted worse prognosis, but also exerted tumor suppressive effects on the proliferation, migration and invasion of NSCLC cells (Yang et al., 2019). Except for these studied lncRNAs, more lncRNAs still need to be explored in the pathogenesis of NSCLC.

Over the past decade, the development of bioinformatics analysis has provided the possibility of identifying more lncRNAs associated with tumor progression. Among these data, a novel antisense lncRNA ATAMTS9-AS1 was initially identified by Wang et al. (2016) who performed lncRNA microarray profiling to find it was involved in malignant epithelial ovarian cancer. Then, Li et al. (2017) found that ADAMTS9-AS1 could significantly stratify esophageal squamous cell carcinoma (ESCC) patients into high-risk

Corresponding Author: Zhongwen Li, Department of Oncology, The Second Affiliated Hospital of Zunyi Medical University, Zunyi, Guizhou, 563000, PR China. e-mail: zhongwen_li080@126.com

DOI: 10.14670/HH-18-347

and low-risk groups, which was much better than traditional clinical tumor markers. Subsequently, ADAMTS9-AS1 has been shown to independently predict overall survival of breast cancer patients by the RNA sequencing data obtained from the Cancer Genome Atlas database (Fan et al., 2018). More recently, bioinformatics analysis further confirmed that ADAMTS9-AS1 was the most remarkable prognostic value and correlated with overall survival in several tumors, including papillary renal cell carcinoma (Liu et al., 2020), bladder cancer (Lin et al., 2020), colon adenocarcinoma (Xing et al., 2018) and prostate cancer (Wan et al., 2019). However, the prognostic value and functional role of ADAMTS9-AS1 in NSCLC still remain elusive.

In the present study, we analyzed the expression level of ADAMTS9-AS1 and its clinical significance in NSCLC patients. After constructing ADAMTS9-AS1 silence-NSCLC cell lines, we performed CCK-8 assay, colony formation, flow cytometry and transwell assay to further explore the functional role of ADAMTS9-AS1 knockdown on NSCLC cell functions. Moreover, we investigated the molecular mechanisms underlying ADAMTS9-AS1 regulating these cellular functions.

Materials and methods

Tissue collection and ethics statement

Human tumor and matched adjacent tissues (at least 5 cm away from the tumor site) were collected from 82 patients diagnosed with NSCLC at the Second Affiliated Hospital of Zunyi Medical University (Guizhou, China) between January 2015 and December 2018. Before surgical resection, no patients received any local or systemic treatment and all signed the informed consent form. The clinicopathologic characteristics of the patients with NSCLC are summarized in Table 1. The follow-up was performed through telephone survey since all patients received surgical resection. All obtained tissue samples were immediately frozen in liquid nitrogen and kept at -80°C until further analysis. The study protocol was in accordance with the Declaration of Helsinki and approved by the Ethics Committee of the Second Affiliated Hospital of Zunyi Medical University.

Cell culture and transfection

Two human NSCLC cell lines (A549 and 95D) were provided by American Type Culture Collection (ATCC, Manassas, VA, USA). A549 cells were grown in Dulbecco's modified Eagle's medium (DMEM) supplemented with 10% fetal bovine serum (Gibco, Grand Island, NY, USA). 95D cells were cultured in RIMI-1640 medium with 10% FBS (Gibco). Both of these cell lines were maintained in a humidified atmosphere of 5% CO_2 at 37°C. For cell transfection, A549 or 95D cells were seeded in six-well plates at a density of 3.0×10^6 cells per well and cultured to 70-80% confluence. Transfection with 100 nM small interfering RNAs targeting ADAMTS9-AS1 (si-ADAMTS9-AS1#1: 5'-GGAATTCAAGCTTCTACAA-3' and si-ADAMTS9-AS1#2: 5'-CCACTGAACACATAAACAT-3') and negative control (si-NC: 5'-UUCUCCGAAC GUGUCACGUTT-3') synthesized by GenePharma Co, Ltd (Shanghai, China) in accordance with Lipofectamine™ 3000 (Invitrogen, Carlsbad, CA, USA). After 48 h transfection, cells were harvested for subsequent experiments.

Real-time quantitative PCR

Total RNA was extracted from tissue samples or cell lines using TRIzol reagent (Invitrogen) and reverse transcribed into complementary DNA (cDNA) with a Prime Script RT Reagent Kit (Takara, Dalian, China). Next, real-time quantitative PCR was carried out on ABI StepOnePlus system (Applied Biosystems, Foster City, CA, USA) using SYBR® Premix Ex Taq™ II kit (Takara) with the following primer sequences: ADAMTS9-AS1 (forward: 5'-TACTGGTTTGGA CATGAGG-3' and reverse: 5'-AAAGGGGTGTTG GCACTC-3') and GAPDH (forward, 5'- GTCTCCT CTGACTTCAACAGCG-3', and reverse, 5'- ACCACC CTGTTGCTGTAGCCAA-3'). Relative fold changes in ADAMTS9-A1 expression were calculated with $2^{-\Delta\Delta Ct}$ method. Each experiment was performed in triplicate and repeated three times.

Table 1. The relationship between ADAMTS9-AS1 expression and clinicopathological characteristics among patients with NSCLC.

Characteristics	Cases (n=82)	ADAMTS9-AS1 expression: High (n=43, median ≤2.834)	ADAMTS9-AS1 expression: Low (n=39, median >2.834)	P-values (chi-square test)
Age				0.298
<60 year	42	25	27	
≥60 year	40	18	12	
Gender				0.763
Male	56	30	26	
Female	26	13	13	
Smoking history				0.669
Yes	57	29	28	
No	35	14	11	
Tumor size				0.017*
<4 cm	49	31	18	
≥4 cm	33	12	21	
TNM stage				0.030*
I/II	52	32	20	
III/IV	30	11	19	
Lymph node metastasis				0.026*
Negative	58	35	23	
Positive	24	8	16	
Pathological type				0.985
Adenocarcinoma	63	33	30	
Squamous carcinoma	19	10	9	

The bold values indicate the P values which are less than 0.05.

Cell counting Kit-8 (CCK-8) assay

Approximately 3.5×10^3 transfected A549 or 95D cells were seeded into each well of 96-well plates and cultured for 0, 24, 48 and 72 h, respectively. Then, 10 μL CCK-8 solution (Dojindo, Kumamoto, Japan) was added to each well. After another 2 h incubation at 37°C, the optical density (OD) value in each well was measured at 450 nm using a microplate reader (Bio-Rad Laboratories, Inc., Hercules, CA, USA). Each experiment was performed in triplicate and repeated three times.

Colony formation assay

Transfected A549 or 95D cells at a density of 500 cells per well were plated in six-well plates and cultured for two weeks to form colonies. The colonies were fixed with 4% paraformaldehyde for 10 min and incubated with 0.1% crystal violet (Sigma-Aldrich). Afterwards, the number of colonies was counted in randomly selected three fields under a light microscope. Each experiment was performed in triplicate and repeated three times.

Flow cytometry analysis

After transfection, A549 or 95D cells were seeded into six-cm dishes at a density of 1.5×10^5 cells per dish and collected until 80% confluence. After fixing with 70% ethanol for 30 min at 4°C, cells were incubated with a propidium iodide (PI, 100 μg/ml) solution containing 10 μg/ml of DNase-free RNase A (Sigma-Aldrich, MO China) for 30 min at room temperature, which were subjected to flow cytometry analysis with a flow cytometer (BD Biosciences, San Jose USA). Apoptosis analysis was performed by Annexin V-FITC/PI Apoptosis Detection Kit (KeyGEN Biotech, Nanjing, China) according to the manufacturer's instructions. Each experiment was performed in triplicate and repeated three times.

Transwell assay

The 24-well Transwell insert (8 μm pore size, Corning, NY, USA) pro-coated without and with Matrigel (BD Biosciences) was used to analyze the cell migration and invasion, respectively. In brief, approximately 5×10^4 transfected A549 or 95D cells in serum -free medium were placed into the upper chamber of a transwell insert. The lower chamber was filled with 500 μL of grown medium with 10% FBS as a chemoattractant. After 24 h of incubation, cells that migrated or invaded to the lower chamber were fixed with 4% paraformaldehyde and stained with 0.1% crystal violet. The stained cells were counted in five random fields under a light microscope (Olympus, Tokyo, Japan) at a 200× magnification. Experiments were independently repeated three times.

Western blot assay

Total protein was obtained by lysing cells with RIPA lysis buffer (Solarbio, Beijing, China), which was quantified by a BCA protein assay kit (Beyotime, Shanghai, China). An equal amount of protein sample (30 μg) was electrophoresed on 10% sodium dodecyl sulfate-polyacrylamide gel electrophoresis (SDS-PAGE) and transferred onto a PVDF membrane (Millipore, Billerica, MA, USA). After being blocked in 5% skim milk in Tris-buffered saline with Tween-20 (TBST) for 2 h, the membranes were incubated with primary antibodies against CDK4, Bad, E-cadherin, N-cadherin, Vimentin and GAPDH overnight at 4°C. Following washing with TBST three times, the membranes were incubated with horseradish peroxidase-conjugated secondary antibodies for 2 h at room temperature. Finally, the protein bands were detected by enhanced chemiluminescence (Thermo Scientific, MA, USA) with GAPDH as a loading control.

Statistical analysis

The statistical analyses were calculated by GraphPad Prism V.6.0. Data were expressed as mean ± SD of three independent experiments. The Chi-squared test was used to evaluate the correlation between ADAMTS9-AS1 expression and clinicopathological parameters in patients with NSCLC. Overall survival (OS) was calculated from the time at diagnosis to the time of death of any cause and compared by Kaplan-Meier method with log-rank test. Cox's regression model was applied for univariate and multivariate analysis. Statistical significance was assessed using the Student's t-test for independent groups. The values of $p<0.05$ were considered to be statistically significant.

Results

ADAMTS9-AS1 was upregulated in NSCLC tissues and associated with the clinicopathological features of NSCLC patients

Real-time quantitative PCR was first performed to investigate the expression of ADAMTS9-AS1 in 82 pairs of NSCLC tissues and matched adjacent tissues. As shown in Fig. 1A, ADAMTS9-AS1 expression level was significantly upregulated in tumor tissues compared with adjacent tissues derived from 82 cases of NSCLC patients. Next, all NSCLC samples were divided into relatively high (above the median, n=43) and low (below the median, n=39) ADAMTS9-AS1 expression groups. The results from Chi-square test indicated that relative higher ADAMTS9-AS1 level was correlated to tumor size (p=0.017), TNM stage (p=0.030) and lymph node metastasis (p=0.026), but was not associated with age, gender, smoking and pathological type (Table 1).

Overexpression of ADAMTS9-AS1 level predicted worse survival prognosis in NSCLC patients

Moreover, we explored the prognostic role of ADAMTS9-AS1 in NSCLC patients. As depicted in Fig. 1B, the median survival time for low ADAMTS9-AS1 expression group was significantly higher than that for high ADAMTS9-AS1 expression group, as determined by Kaplan–Meier analysis and log-rank test. We further confirmed the prognostic role of ADAMTS9-AS1 in NSCLC patients by performing the univariate and multivariate survival analysis based on Cox proportional hazards regression model. As shown in Table 2, ADAMTS9-AS1 expression could be regarded as an independent predictor for overall survival in patients with NSCLC (p=0.007), as well as TNM stage (p=0.015) and lymph node metastasis (p=0.031).

Knockdown of ADAMTS9-AS1 impaired NSCLC cell proliferation, induced cell cycle arrest and apoptosis in vitro

Since the expression of ADAMTS9-AS1 was confirmed to be upregulated in NSCLC tissues, we wanted to explore whether downregulation of ADAMTS9-AS1 could suppress the progression of NSCLC. Here, two different siRNAs (si-ADAMTS9-AS1#1 and si-ADAMTS9-AS1#2) were used to transfect two NSCLC cell lines (A549 and 95D) to silence ADAMTS9-AS1 expression. At 48 h post-transfection, real time quantitative PCR demonstrated that the expression of ADAMTS9-AS1 was significantly

Table 2. Univariate and multivariate analysis of NSCLC patients on overall survival.

Characteristic	HR (95% CI)	P-value
Univariate analysis		
Age (years: <60 vs. ≥60)	1.085 (0.721-1.885)	0.645
Gender (Male vs. Female)	1.456 (0.912-2.132)	0.152
Smoking history (Yes vs. No)	1.412 (0.965-2.213)	0.124
Tumor size (cm: <4 vs. ≥4)	0.543 (0.268-1.225)	0.010*
TNM stage (I/II vs. III/IV)	3.012 (1.668-5.124)	0.008*
Lymph node metastasis (Negative vs. Positive)	1.962 (1.254-2.865)	0.035*
Pathological type (Adenocarcinoma vs. Squamous carcinoma)	1.248 (0.745-2.435)	0.385
Multivariate analysis		
Tumor size (cm: <4 vs. ≥4)	0.778 (0.524-1.235)	0.331
TNM stage (I/II vs. III/IV)	2.284 (1.168-4.052)	0.015*
Lymph node metastasis (Negative vs. Positive)	1.372 (0.865-2.312)	0.031*
ADAMTS9-AS1 expression (High vs. Low)	3.698 (2.256-5.623)	0.007*

*p<0.05. Abbreviations: NSCLC, non-small cell lung cancer; LNM, lymph node metastasis; HR, hazard ratio; CI, confidence interval.

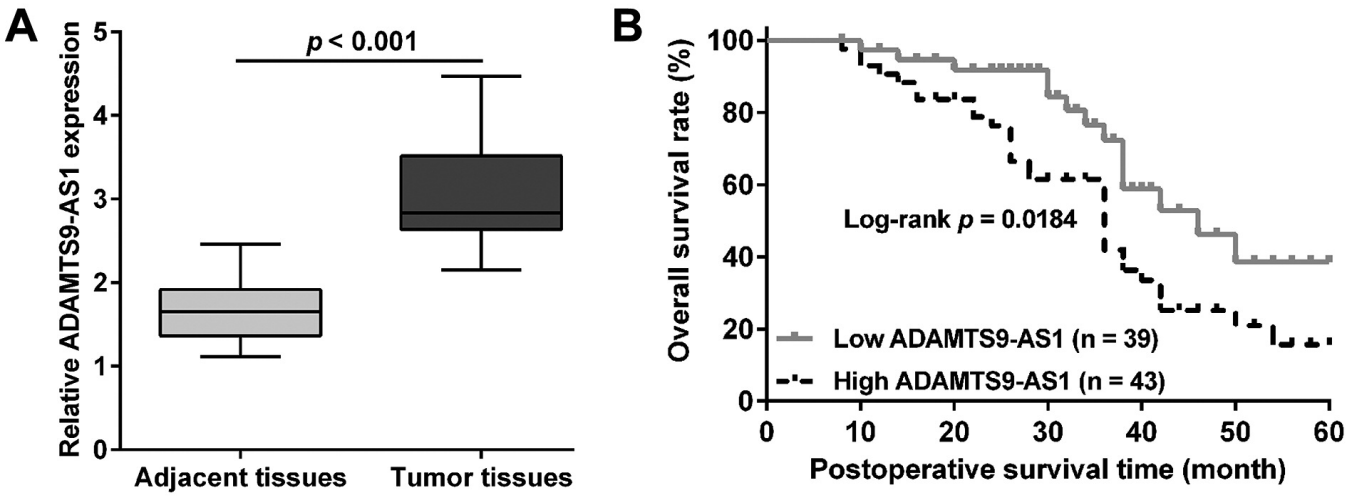

Fig. 1. The expression and prognostic role of ADAMTS9-AS1 in human non-small cell lung cancer (NSCLC) patients. **A.** Relative expression levels of ADAMTS9-AS1 in NSCLC tissues (n=82) compared with corresponding matched adjacent tissues (n=82). ADAMTS9-AS1 expression was examined using real time quantitative PCR and was normalized to GAPDH expression. **B.** Kaplan-Meier overall survival (OS) curves according to high and low ADAMTS9-AS1 expression levels.

downregulated after either si-ADAMTS9-AS1#1 or si-ADAMTS9-AS1#2 transfection compared with si-NC transfection in both A549 and 95D cells (Fig. 2A). Notably, si-ADAMTS9-AS1#1 had stronger suppressive effects on ADAMTS9-AS1 expression than si-ADAMTS9-AS1#2, which was thus selected for the subsequent experiments. CCK-8 assay showed that knockdown of ADAMTS9-AS1 remarkedly suppressed cell viability and growth of A549 (Fig. 2B) and 95D (Fig. 2C) cells. Similarly, the results of the colony formation assay revealed that knockdown of ADAMTS9-AS1 greatly attenuated the proliferation ability of A549 and 95D cells, as reflected by decreased colonies in si-ADAMTS9-AS1#1 group compared with si-NC group (Fig. 2D). Next, flow cytometric analysis was performed to examine the effects of ADAMTS9-AS1 on the cell cycle progression and apoptosis of NSCLC cells. As shown in Fig. 3A, the percentage of cells at G0/G1 phase was significantly increased, along with reduced cell proportion at G2/M phase in A549 and 95D cells after ADAMTS9-AS1 knockdown, which implied that ADAMTS9-AS1 knockdown caused cell cycle G0/G1 phase arrest in NSCLC cells. Furthermore, si-ADAMTS9-AS1#1 transfection notably promoted cell early and late apoptosis in both A549 and 95D cells (Fig. 3B).

Knockdown of ADAMTS9-AS1 inhibited the migration and invasion of NSCLC cells in vitro

Additionally, we evaluated the effects of ADAMTS9-AS1 on the migration and invasion ability of NSCLC cells using transwell assay. As shown in Fig. 4A, the number of migratory cells was significantly decreased in si-ADAMTS9-AS1#1 group compared with si-NC group in A549 (si-ADAMTS9-AS1#1 vs. si-NC: 33.3±4.2 vs. 86.3±4.5) and 95D (si-ADAMTS9-AS1#1 vs. si-NC: 55.0±4.6 vs. 108.0±4.0) cells. Similarly, ADAMTS9-AS1 knockdown significantly reduced the number of invasive cells from 73.7±4.0 to 21.7±3.5 in A549 cells and from 96.3±4.0 to 33.3±3.2 in 95D cells (Fig. 4B). These results suggested that knockdown of ADAMTS9-AS1 had a negative effect on cell migration and invasion in NSCLC.

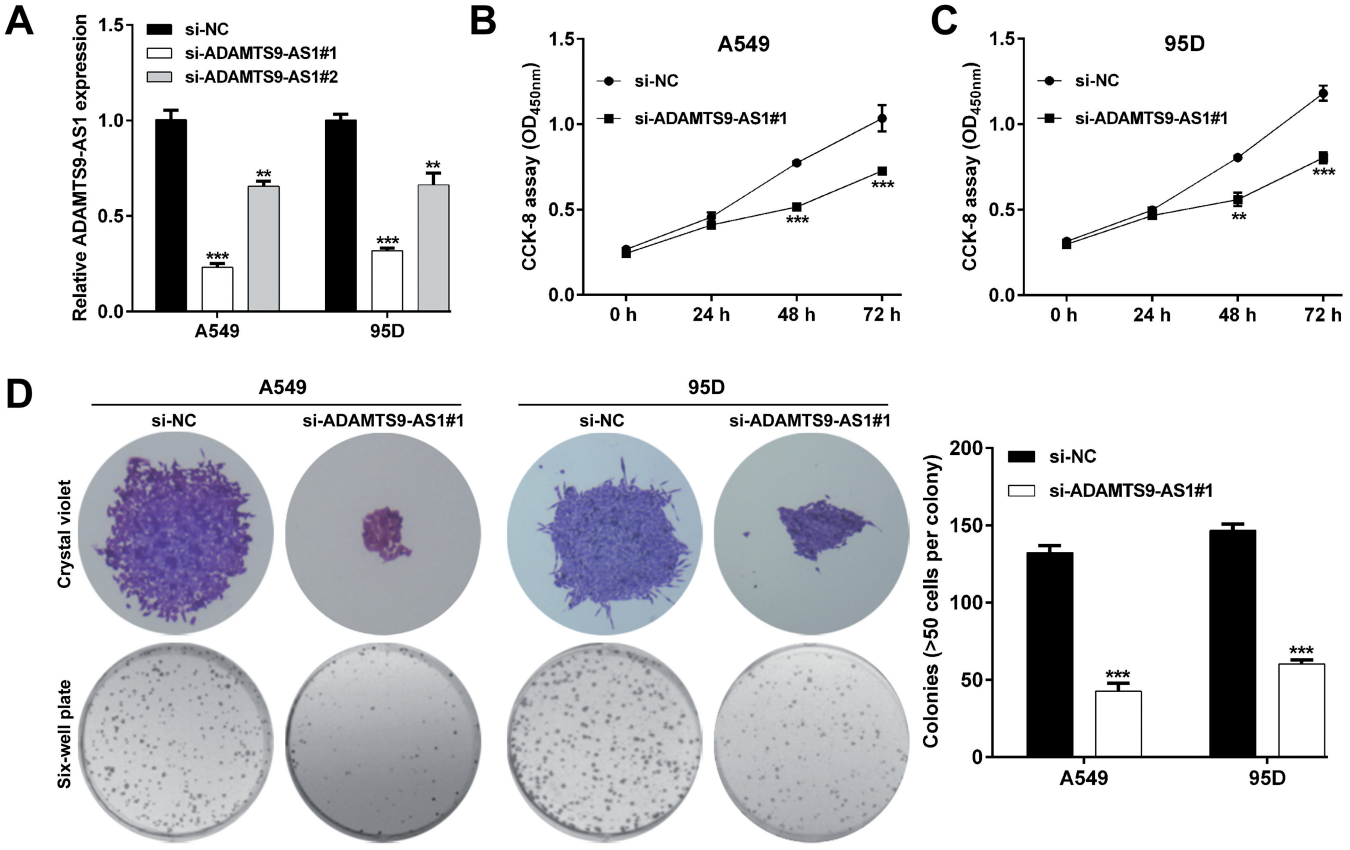

Fig. 2. Effects of ADAMTS9-AS1 knockdown on NSCLC cell proliferation *in vitro*. **A.** The relative expression levels of ADAMTS9-AS1 in A549 and 95D cells transfected with si-NC or si-ADAMTS9-AS1 (si-ADAMTS9-AS1#1 and si-ADAMTS9-AS1#2) were measured using real time quantitative PCR. **B, C.** CCK-8 assay was performed to determine the cell viability of the transfected A549 and 95D cells. **D.** Colony-forming assay was conducted to determine the proliferation of the transfected A549 and 95D cells. The colonies were counted and captured. Data are expressed as mean ± SD of three independent experiments. **p<0.01, ***p<0.001, compared with si-NC.

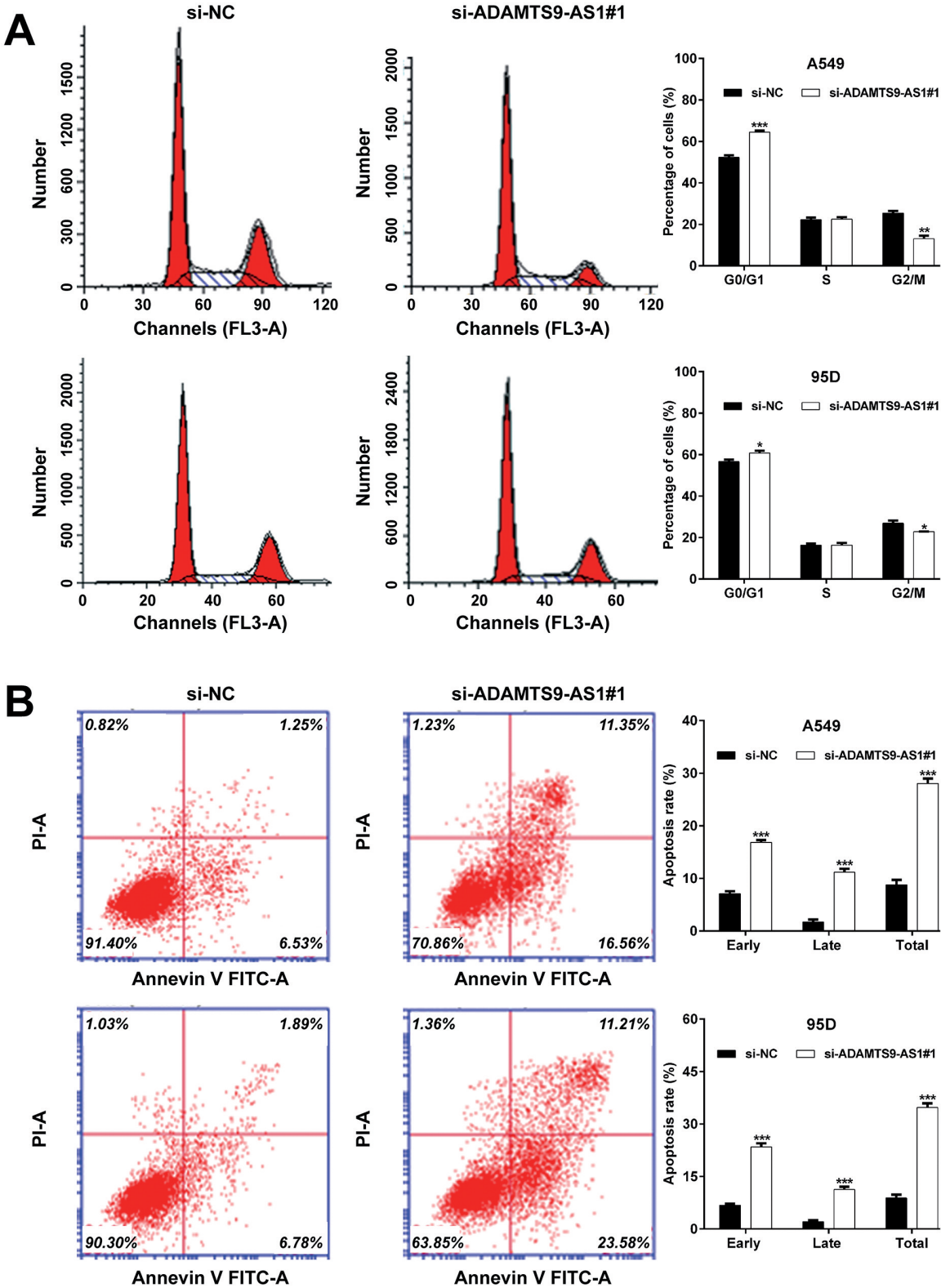

Fig. 3. Effects of ADAMTS9-AS1 knockdown on NSCLC cell cycle progression and apoptosis *in vitro*. **A.** Cell cycle distribution was analyzed by flow cytometry with PI staining in A549 and 95D cells after transfection with si-ADAMTS9-AS1#1 or si-NC. **B.** Cell apoptosis was analyzed by flow cytometry with Annexin V/PI staining in A549 and 95D cells after transfection with si-ADAMTS9-AS1#1 or si-NC. Data are expressed as mean ± SD of three independent experiments. ***p<0.001, compared with si-NC.

Knockdown of ADAMTS9-AS1 affected the proliferation and EMT-related protein expression in NSCLC cells

To further explore the molecular mechanisms underlying ADAMTS9-AS1 knockdown regulating NSCLC cell proliferation, migration and invasion, western blot analysis was performed to detect the protein levels of G1/S transition, apoptosis and EMT process. As shown in Fig. 5A, obviously downregulated CDK4, N-cadherin and Vimentin, as well as upregulated Bad and E-cadherin were found in the si-ADAMTS9-AS1#1 group compared with the si-NC group in A549 cells. Consistently, ADAMTS9-AS1 knockdown decreased the protein expression of CDK4, N-cadherin and Vimentin, while it increased the protein expression of Bad and E-cadherin in 95D cells (Fig. 5B).

Discussion

Here, we observed that ADAMTS9-AS1 expression was significantly upregulated in tumor tissues compared with matched adjacent tissues derived from 82 cases of NSCLC patients. Further analysis showed that highly

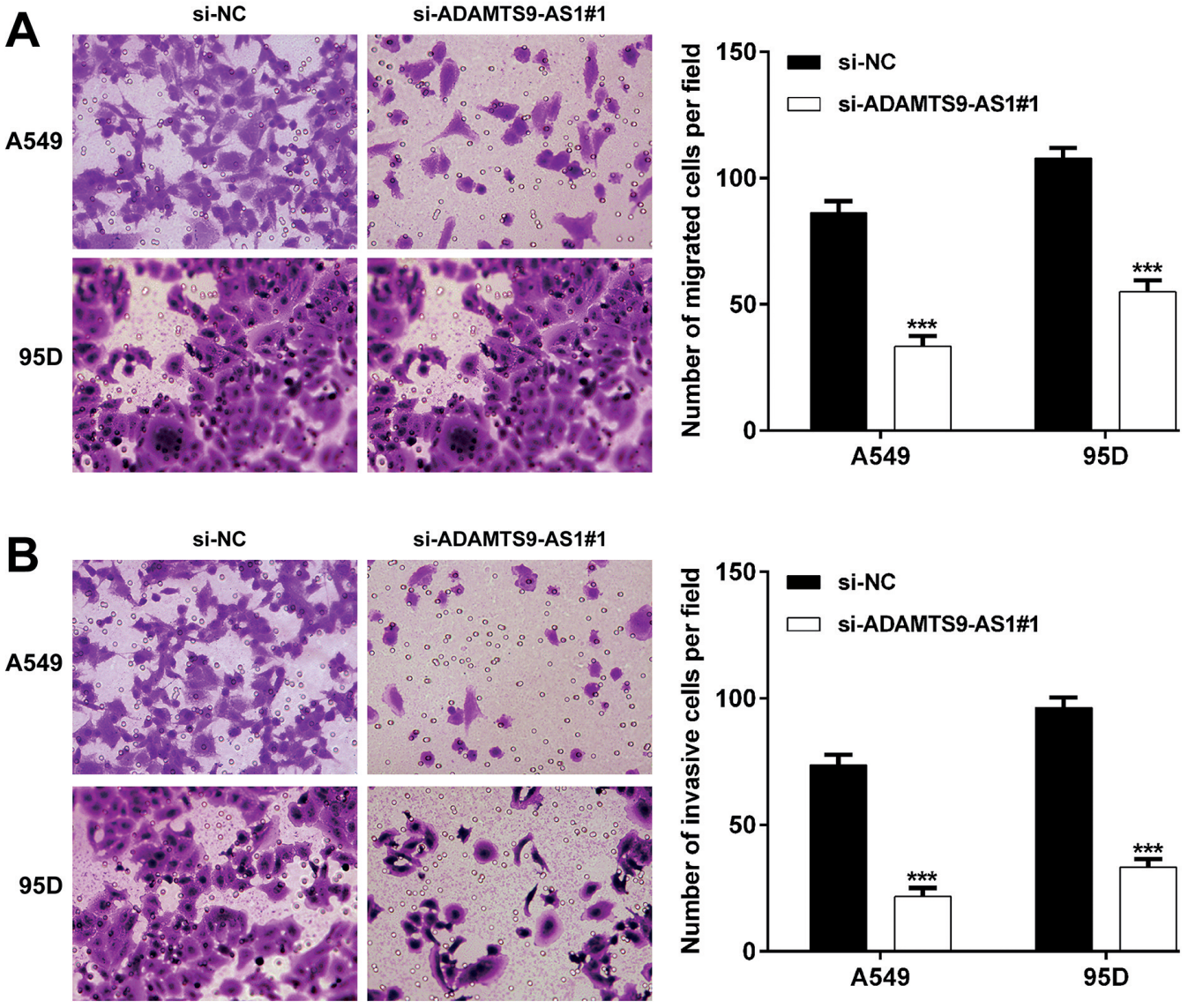

Fig. 4. Effects of ADAMTS9-AS1 knockdown on NSCLC cell migration and invasion *in vitro*. Transwell assay was performed to evaluate cell migration **(A)** and invasion **(B)** in A549 and 95D cells after transfection with si-ADAMTS9-AS1#1 or si-NC. Representative images of migratory and invasive cells are shown in left panel and quantification of migratory and invasive cells are displayed in right panel. Data are expressed as mean ± SD of three independent experiments. ***p<0.001, compared with si-NC.

expressed ADAMTS9-AS1 was associated with tumor size, TNM stage and lymph node metastasis, as well as predicting worse survival prognosis in NSCLC patients. Moreover, Cox's regression model analysis indicated that ADAMTS9-AS1 served as an independent prognostic marker for overall survival in patients with NSCLC. These clinical analyses suggested that ADAMTS9-AS1 might be an oncogene participating in the initiation and development mechanisms of NSCLC. In agreement with our data, ADAMTS9-AS1 expression was higher in hepatocellular carcinoma (HCC) cell lines compared to normal cells (Zhang et al., 2020). The overall survival and disease-free survival were significantly shorter in patients with high ADAMTS9-AS1 bladder cancer (Xu et al., 2019a,b; Lin et al., 2020). On the contrary, ADAMTS9-AS1 expression was notably decreased and functioned as a novel prognostic biomarker associated with overall survival in breast cancer (Fan et al., 2018) and colon adenocarcinoma (Xing et al., 2018). ADAMTS9-AS1 was downregulated in breast cancer tissues as well as cell lines (Fang et al., 2020). Li et al. (2020) identified that ADAMTS9-AS1 was significantly decreased in colorectal cancer tissues and correlated with clinical outcome of patients according to The Cancer Genome Atlas (TCGA) database. These controversies the clinical significance of ADAMTS9-AS1 made us conclude that different tumor types and sample size might be the major reasons explaining the opposite prognostic value of ADAMTS9-AS1.

Subsequently, the functional role of ADAMTS9-AS1 in NSCLC cells was examined *in vitro*. Our data showed that depletion of ADAMTS9-AS1 significantly suppressed cell proliferation, migration, and induced cell cycle G0/G1 phase arrest and apoptosis in both A549 and 95D cells. A similar oncogenic role of ADAMTS9-AS1 has been reported in several tumors. For instance, Zhang et al. (2020) revealed that ADAMTS9-AS1 contributed to proliferation, migration, and invasion in HCC cells. Depletion of ADAMTS9-AS1 significantly suppressed cell proliferation, G1/S transition, migration and invasion in colorectal cancer cells (Chen et al., 2020). Opposite to our data, Wan et al. (2019) found that ADAMTS9-AS1 significantly influences tumor cell growth and proliferation, suggesting that it plays a tumor suppressive role in prostate cancer. Upregulation of ADAMTS9-AS1 suppressed the growth and invasiveness of breast carcinoma cells *in vitro* as well as inhibiting cell growth *in vivo* (Fang et al., 2020). ADAMTS9-AS1 suppressed cell proliferation and migration both *in vitro* and *in vivo* in colorectal cancer (Li et al., 2020). The oncogenic or tumor suppressive role of ADAMTS9-AS1 mainly depends on different tumor types. To further confirm the accelerative effects of ADAMTS9-AS1 on NSCLC cell proliferation and metastasis *in vitro*, we examined the related protein

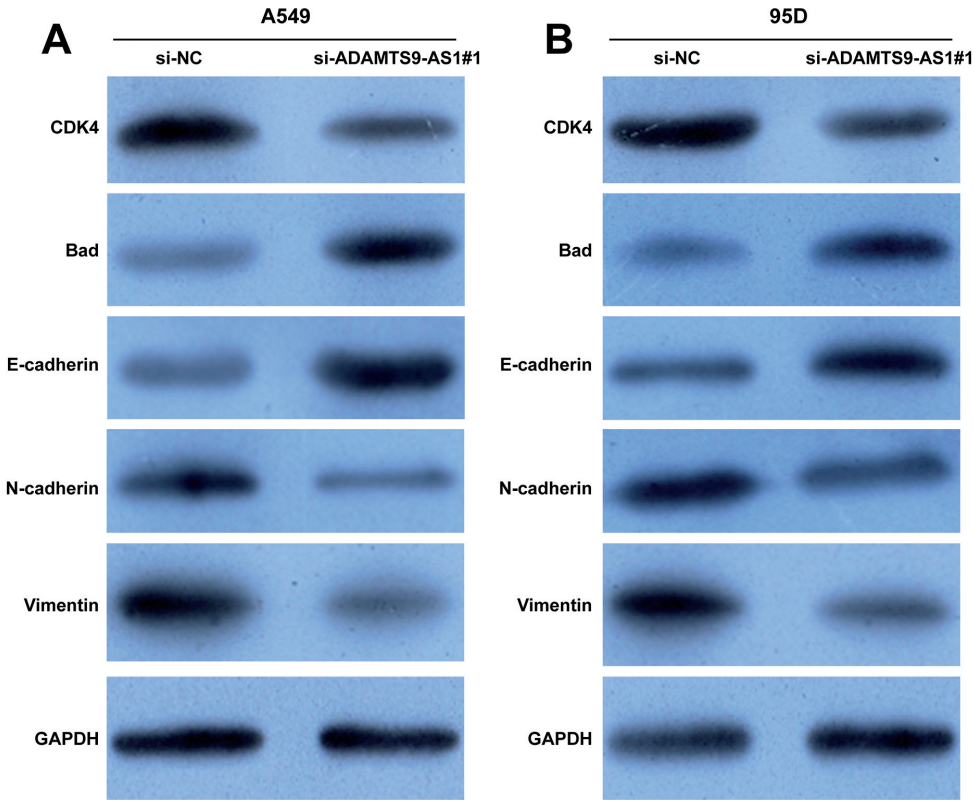

Fig. 5. Knockdown of ADAMTS9-AS1 affected the proliferation and EMT-related protein expression in NSCLC cells. Western blot analysis was performed to detect the protein expression of CDK4, Bad, E-cadherin, N-cadherin and Vimentin in A549 **(A)** and 95D **(B)** cells after transfection with si-ADAMTS9-AS1#1 or si-NC.

markers. As expected, knockdown of ADAMTS9-AS1 downregulated the expression of CDK4, N-cadherin, Vimentin and upregulated the expression of Bad and E-cadherin in both A549 and 95D cells. To our best knowledge, abnormal tumor cell proliferation is closely associated with regulation of the cell cycle which depends on the precise coordination of cyclin-dependent kinases (CDKs) and cyclins (Malumbres, 2011), of which CDK4 is one of the key regulators in G1/S cell cycle transition (Ding et al., 2020). In addition to cell cycle progression, apoptosis, a process of programmed cell death, plays an important role in regulating cell proliferation, of which BCL-2 family proteins are essential in modulating apoptosis status, including Bad as a pro-apoptotic BH3-only protein (Denault and Boatright, 2004; Kale et al., 2018). Here, we speculated that ADAMTS9-AS1 knockdown induced impaired growth and proliferation of NSCLC cells might be ascribed to its regulation on decreased CDK4 and increased Bad expression. In addition, tumor metastasis is another primary characteristic of cancer, including the classical epithelial mesenchymal transition (EMT) theory in recent years (Ombrato and Malanchi, 2014). The EMT process is characterized by increased migration ability and invasiveness, which was correlated with downregulation of epithelial marker E-cadherin and upregulation of mesenchymal markers, such as N-cadherin and vimentin (Miettinen et al., 1994; Kalluri and Weinberg, 2009). In line with the decreased migration and invasion ability, knockdown of ADAMTS9-AS1 promoted E-cadherin, while suppressing the expression of N-cadherin and Vimentin in NSCLC cells. Notably, the observation in the study of Chen et al. is very similar to our data which indicated that depletion of ADAMTS9-AS1 significantly suppressed cell proliferation, G1/S transition, migration and invasion, and also suppressed CDK4/Cyclin D1 and epithelial-mesenchymal transition (EMT) in colorectal cancer (Chen et al., 2020).

In fact, the crosstalk between lncRNAs and miRNAs is common in cancer biology (Yu et al., 2017). To our best knowledge, ADAMTS9-AS1 related miRNA sponge regulatory network has been identified and analyzed in bladder urothelial carcinoma (Wang et al., 2019) and breast cancer (Tuersong et al., 2019). Functionally, lncRNA ADAMTS9-AS1 inhibited the aggressive phenotypes of breast carcinoma cells via sponging miR-513a-5p and regulating ZFP36 (Fang et al., 2020). Here, lacking of the study on the association between ADAMTS9-AS1 and mRNAs via certain miRNA was one of the limitations in our study.

In summary, we found that high ADAMTS9-AS1 expression predicted worse overall survival for NSCLC patients. Knockdown of ADAMTS9-AS1 was able to suppress the development of progression of NSCLC via suppressing cell proliferation, migration, invasion and EMT. The findings of the present study indicate that ADAMTS9-AS1 may serve as a potential therapeutic target for the treatment of patients with NSCLC.

Ethics approval and consent to participate. All the patients in the present study provided written informed consent. The present study was approved by The Ethics Committee of The Second Affiliated Hospital of Zunyi Medical University (approval no. SAH-2018-2301).

Availability of data and materials. The datasets used and/or analyzed during the present study are available from the corresponding author on reasonable request.

Authors' contributions. LZW designed the current study. YGJ and ZTY performed the experiments and analyzed the data. WJZ drafted the manuscript. WJZ and TX wrote the manuscript. All authors read and approved the final manuscript.

Funding. This work was supported by National Natural Science Foundation of China Grants (no. 81860441) and Guizhou Province Science and Technology Cooperation (no. LH [2015]7486).

Consent for publication. Not applicable.

Competing interests. The authors declare that they have no competing interests.

References

Cai Z. and Liu. Q (2019). Understanding the global cancer statistics 2018: Implications for cancer control. Sci. China Life Sci. 64, 1017-1020.

Chen W., Tu Q., Yu L., Xu Y., Yu G., Jia B., Cheng Y. and Wang Y. (2020). LncRNA ADAMTS9-AS1, as prognostic marker, promotes cell proliferation and EMT in colorectal cancer. Hum. Cell 33, 1133-1141.

Chen X. and Wang K. (2019). LncRNA ZEB2-AS1 aggravates progression of non-small cell lung carcinoma via suppressing pten level. Med. Sci. Monit. 25, 8363-8370.

Crino L., Weder W., van Meerbeeck J., Felip E. and Group E.G.W. (2010). Early stage and locally advanced (non-metastatic) non-small-cell lung cancer: Esmo clinical practice guidelines for diagnosis, treatment and follow-up. Ann. Oncol. 21 (Suppl. 5), v103-115.

Denault J.B. and Boatright K. (2004). Apoptosis in biochemistry and structural biology. 3-8 february 2004, keystone, co, USA. IDrugs. 7, 315-317.

Didkowska J., Wojciechowska U., Manczuk M. and Lobaszewski J. (2016). Lung cancer epidemiology: Contemporary and future challenges worldwide. Ann. Transl. Med. 4, 150.

Ding J., Xu K., Sun S., Qian C., Yin S., Xie H., Zhou L., Zheng S. and Zhang W. (2020). SOCS1 blocks G1-S transition in hepatocellular carcinoma by reducing the stability of the CyclinD1/CDK4 complex in the nucleus. Aging (Albany NY). 12, 3962-3975.

Fan C.N., Ma L. and Liu N. (2018). Systematic analysis of lncRNA-miRNA-mRNA competing endogenous RNA network identifies four-lncRNA signature as a prognostic biomarker for breast cancer. J. Transl. Med. 16, 264.

Fang S., Zhao Y. and Hu X. (2020). LncRNA ADAMTS9-AS1 restrains the aggressive traits of breast carcinoma cells via sponging mir-513a-5p. Cancer Manag. Res. 12, 10693-10703.

Hirsch F.R., Scagliotti G.V., Mulshine J.L., Kwon R., Curran W.J. Jr, Wu Y.L. and Paz-Ares L. (2017). Lung cancer: Current therapies and new targeted treatments. Lancet 389, 299-311.

Hui B., Ji H., Xu Y., Wang J., Ma Z., Zhang C., Wang K. and Zhou Y. (2019). RREB1-induced upregulation of the lncRNA AGAP2-AS1 regulates the proliferation and migration of pancreatic cancer partly

through suppressing ankrd1 and ANGPTL4. Cell Death Dis. 10, 207.

Kale J., Osterlund E.J. and Andrews D.W. (2018). Bcl-2 family proteins: Changing partners in the dance towards death. Cell Death Differ. 25, 65-80.

Kalluri R. and Weinberg R.A. (2009). The basics of epithelial-mesenchymal transition. J. Clin. Invest. 119, 1420-1428.

Li Z., Yao Q., Zhao S., Wang Y., Li Y. and Wang Z. (2017). Comprehensive analysis of differential co-expression patterns reveal transcriptional dysregulation mechanism and identify novel prognostic lncRNAs in esophageal squamous cell carcinoma. Onco Targets Ther. 10, 3095-3105.

Li N., Li J., Mi Q., Xie Y., Li P., Wang L., Binang H., Wang Q., Wang Y., Chen Y., Wang Y., Mao H., Du L. and Wang C. (2020). Long non-coding RNA ADAMTS9-AS1 suppresses colorectal cancer by inhibiting the Wnt/beta-catenin signalling pathway and is a potential diagnostic biomarker. J. Cell Mol. Med. 24, 11318-11329.

Lin Y.Z., Wu Y.P., Ke Z.B., Cai H., Chen D.N., Chen S.H., Li X.D., Lin T.T., Huang J.B., Zheng Q.S., Xue X.Y., Xu N. and Wei Y. (2020). Bioinformatics analysis of the expression of key long intergenic non-protein coding RNA genes in bladder cancer. Med. Sci. Monit. 26, e920504.

Liu Y., Gou X., Wei Z., Yu H., Zhou X. and Li X. (2020). Bioinformatics profiling integrating a four immune-related long non-coding RNAs signature as a prognostic model for papillary renal cell carcinoma. Aging (Albany NY). 12, 15359-15373.

Malumbres M (2011). Physiological relevance of cell cycle kinases. Physiol. Rev. 91, 973-1007.

Miettinen P.J., Ebner R., Lopez A.R. and Derynck R. (1994). TGF-beta induced transdifferentiation of mammary epithelial cells to mesenchymal cells: Involvement of type i receptors. J. Cell Biol. 127, 2021-2036.

Ombrato L. and Malanchi I. (2014). The EMT universe: Space between cancer cell dissemination and metastasis initiation. Crit. Rev. Oncog. 19, 349-361.

Pao W. and Chmielecki J. (2010). Rational, biologically based treatment of egfr-mutant non-small-cell lung cancer. Nat. Rev. Cancer 10, 760-774.

Qu C.X., Shi X.C., Zai L.Q., Bi H. and Yang Q. (2019). LncRNA CASC19 promotes the proliferation, migration and invasion of non-small cell lung carcinoma via regulating miRNA-130b-3p. Eur. Rev. Med. Pharmacol. Sci. 23, 247-255.

Tuersong T., Li L., Abulaiti Z. and Feng S. (2019). Comprehensive analysis of the aberrantly expressed lncRNA-associated ceRNA network in breast cancer. Mol. Med. Rep. 19, 4697-4710.

Wan J., Jiang S., Jiang Y., Ma W., Wang X., He Z., Wang X. and Cui R. (2019). Data mining and expression analysis of differential lncRNA ADAMTS9-AS1 in prostate cancer. Front Genet. 10, 1377.

Wang H., Fu Z., Dai C., Cao J., Liu X, Xu J., Lv M., Gu Y., Zhang J., Hua X., Jia G., Xu S., Jia X. and Xu P. (2016). LncRNAs expression profiling in normal ovary, benign ovarian cyst and malignant epithelial ovarian cancer. Sci. Rep. 6, 38983.

Wang J., Zhang C., Wu Y., He W. and Gou X. (2019). Identification and analysis of long non-coding RNA related miRNA sponge regulatory network in bladder urothelial carcinoma. Cancer Cell Int. 19, 327.

Xing Y., Zhao Z., Zhu Y., Zhao L., Zhu A. and Piao D. (2018). Comprehensive analysis of differential expression profiles of mRNAs and lncRNAs and identification of a 14-lncRNA prognostic signature for patients with colon adenocarcinoma. Oncol. Rep. 39, 2365-2375.

Xu C.H., Xiao L.M., Liu Y., Chen L.K., Zheng S.Y., Zeng E.M. and Li D.H. (2019a). The lncRNA HOXA11-AS promotes glioma cell growth and metastasis by targeting miR-130a-5p/HMGB2. Eur. Rev. Med. Pharmacol. Sci. 23, 241-252.

Xu Z., Wang C., Xiang X., Li J. and Huang J. (2019b). Characterization of mRNA expression and endogenous RNA profiles in bladder cancer based on the cancer genome atlas (TCGA) database. Med. Sci. Monit. 25, 3041-3060.

Yang Y., Chen D., Liu H. and Yang K. (2019). Increased expression of lncRNA CASC9 promotes tumor progression by suppressing autophagy-mediated cell apoptosis via the akt/mtor pathway in oral squamous cell carcinoma. Cell Death Dis. 10, 41.

Yu Y., Nangia-Makker P., Farhana L. and Majumdar A.P.N. (2017). A novel mechanism of lncRNA and miRNA interaction: CCAT2 regulates miR-145 expression by suppressing its maturation process in colon cancer cells. Mol. Cancer 16, 155.

Zhang Z., Li H., Hu Y. and Wang F. (2020). Long non-coding RNA ADAMTS9-AS1 exacerbates cell proliferation, migration, and invasion via triggering of the Pi3K/AKT/mTOR pathway in hepatocellular carcinoma cells. Am. J. Transl. Res. 12, 5696-5707.

Accepted June 4, 2021